Published online 11 June 2010 *Nucleic Acids Research, 2010, Vol. 38, Web Server issue* ***W641–W646***
doi:10.1093/nar/gkq542

ParticleStats: open source software for the analysis of particle motility and cytoskeletal polarity

Russell S. Hamilton*, Richard M. Parton, Raquel A. Oliveira, Georgia Vendra, Graeme Ball, Kim Nasmyth and Ilan Davis

Department of Biochemistry, University of Oxford, South Parks Road, Oxford, OX1 3QU, UK

Received January 19, 2010; Revised May 21, 2010; Accepted May 28, 2010

ABSTRACT

The study of dynamic cellular processes in living cells is central to biology and is particularly powerful when the motility characteristics of individual objects within cells can be determined and analysed statistically. However, commercial programs only offer a limited range of inflexible analysis modules and there are currently no open source programs for extensive analysis of particle motility. Here, we describe ParticleStats (http://www.ParticleStats.com), a web server and open source programs, which input the *X*,*Y* coordinate positions of objects in time, and output novel analyses, graphical plots and statistics for motile objects. ParticleStats comprises three separate analysis programs. First, ParticleStats: Directionality for the global analysis of polarity, for example microtubule plus end growth in *Drosophila* oocytes. Second, ParticleStats:Compare for the analysis of saltatory movement in terms of runs and pauses. This can be applied to chromosome segregation and molecular motor-based movements. Thirdly ParticleStats:Kymographs for the analysis of kymograph images, for example as applied to separation of chromosomes in mitosis. These analyses have provided key insights into molecular mechanisms that are not possible from qualitative analysis alone and are widely applicable to many other cell biology problems.

INTRODUCTION

Live cell imaging of dynamic cellular components has become a central method in Biology. The quantification and analysis of the resulting images allows very powerful dissection of the mechanisms underlying dynamic cellular processes. Statistical analysis of the resulting data is often required to reach clear conclusions regarding the likely mechanisms of motility. One field that has used such an approach extensively, is the study of the mechanism of molecular motor driven transport of cytoplasmic components, such mitochondria (1), lipid droplets (2), *Xenopus* melanocytes (3) and RNA particles (4–7). Particle tracking algorithms are used to track the movement of fluorescently labelled objects over time, resulting in *X* and *Y* coordinates as a function of time (8,9), and are able to output a variety of data, such as speed, direction and run lengths (10). While these parameters are sufficient for some applications, it is often essential to perform more sophisticated specific analyses to generate appropriate parameters for a given type of experiment.

We have developed ParticleStats to perform analyses on *X*, *Y* coordinates describing the motion of a variety of kinds of objects within cells; yielding insights into molecular mechanisms that would not be possible from qualitative analysis alone. First, ParticleStats:Directionality maps globally intracellular polarity or directionality of particle movements. We developed new methods for analysing, displaying and statistically evaluating the overall directionality and polarity of fields of microtubules in cells, as described by the growth of the plus ends of microtubules in living cells. Second, we have developed ParticleStats:Compare for the analysis, display and statistical evaluation of saltatory motility of objects, by comparing, for example, the movements of wild type and mutant particles. We successfully applied the method to RNA particle localization in *Drosophila* (11). Finally, ParticleStats:Kymographs provides novel analysis tools and displays of kymograph images. We successfully applied the method to sister chromatid separation in *Drosophila* blastoderm embryos (12). These tools are provided as a web server and as open source programs available at www.ParticleStats.com.

*To whom correspondence should be addressed. Tel: +44 01865 613271; Fax: +44 01865 613340; Email: russell.hamilton@bioch.ox.ac.uk
Present address:
Georgia Vendra, Center for Brain Research, Medical University of Vienna, Spitalgasse 4, A-1090 Vienna, Austria.

METHODS

ParticleStats:Directionality

The majority of eukaryotic cells are highly polarized, as manifested by their asymmetric morphology and localized distribution of proteins and mRNA. The ParticleStats directionality method was developed to analyse the polarization of the MT network. Setting up a distinct microtubule polarity is the key symmetry breaking event in the *Drosophila* oocyte responsible for asymmetric localization of mRNA and proteins to set up the primary body axes. Our method for mapping overall MT polarity first rotates the time lapse movies according to a user-specified axis, so that they are all consistently aligned (Figure 1A). To provide a visual means of assessing the directionality of a population of particles we created a windmap style representation of net bias. This is achieved by dividing the images into an array of squares, ranging in number from 1 to 4096. Each track is converted to a vector describing its length and direction and is assigned to a specific square or number of squares in the array. A single resultant vector is calculated for each square by summing up the vectors representing all the tracks that cross the square. The resultant vector then provides the direction for that particular square, and the colour intensity of the square is proportional to the number of tracks or magnitude of the vector (Figure 1B). Rose diagrams/circular histograms are plotted to summarize an entire population or sub-population of tracks. The angles of individual tracks are plotted on the circumference of the rose diagram. The petals of the rose diagrams are calculated by summing the number or magnitude of all the tracks travelling in a particular angle range (Figure 1C). To assess the directionality of subregions of images, we have provided the option of only considering tracks crossing a region of interest (ROI). This ROI is provided as a list of polygon vertices by the user and can be any shape or size. We also provide a simple graphical tool for creating ROI coordinates (Figure 1D). To determine if a population of particles has a directionality bias, we have utilized circular statistics and implemented the Watson's test of uniformity, which compares against a Uniform distribution and the von Mises distribution (13). The von Mises distribution is a special case of the normal distribution for circular data.

ParticleStats:Compare

The transport of mRNA by molecular motors is a key mechanism for axis specification in development; fluorescently labelled mRNAs are transported by the molecular motors and can be tracked over time (11,14,15). ParticleStats:Compare aids the determination of the mechanistic basis of molecular motor based movements through detailed analysis of the frequency of runs and pauses. X and Y coordinates are used to determine runs as well as frequency and statistics of pausing. The directions of the runs are determined when an orientation axis is provided, allowing the image to be rotated to this axis. The linear regression method of least squares was used to fit a linear model to a set of data to determine the closeness of fit of the data to the model. This coefficient of determination (r^2) measures the proportion of the data that can be accounted for (Figure 2A and B). The r^2 coefficient also determines whether a particle can reasonably be assumed to be travelling in one direction along a single microtubule. Runs are further divided up into overlapping three frame segments and the segment speeds determined (Figure 2C) in addition to maximum speeds for the run segments (Figure 2D). The directionality of the runs are plotted onto rose diagrams to show if the kinetochore separations are directed rather than showing less directed lateral movements with respect to the user supplied orientation axis (Figure 2E). The frequency of changes in direction of the movements were also determined to provide further insight into the separation dynamics (Figure 2F). Plots of runs for two populations of particles reveal whether there are differences in the distribution of run lengths and speeds. The direction a particle travels in most frequently, the average run lengths and frequency of pauses can all be determined easily and provide insight into the molecular motors involved in the transport. We also successfully applied ParticleStats:Compare to the separation of sister chromatids in mitosis (12).

ParticleStats:Kymographs

Kymographs are a 2D graphical representation of the changes in one spatial dimension with time. ParticleStats:Kymographs was developed to analyse kymographs depicting chromosome separation during cell division (12). During mitosis, individual sister chromatids move apart to opposite poles of the cell, to allow efficient separation of the DNA into two genetically identical sets. Instead of tracking individual centromeres, kymographs show the averaged movement of all centromeres. Each kymograph was treated as two halves for the left and right kinetochores, and the pixel intensity values were extracted for each time point. A weighted average calculation was used to determine the average separation distance for each of the halves of the image (Figure 3A and B). The noise levels were estimated using the edge pixel values with an additional customizable threshold of 95% of the maximum intensity above noise. We implemented a further noise estimation method, a diagonal edge-based pixel measure, where pixels are taken from a diagonal line from the top centre of the image to the bottom right. This second method improves noise estimation in the kinetochore separation kymographs, as the intensities are also mainly on a diagonal. The weighted average distances and weighed standard deviations are plotted on the kymographs for visual inspection, then a user-defined time range is used to calculate the speeds of the kinetochore separation. Linear regression is used to calculate the best fitting line for the distances over the specified time range (Figure 3A and B). Speeds are calculated for each half of the kymograph as well as an overall average speed. This average speed is used to account for any possible misalignment in the two halves of the kymograph. The weighted average distances for each of the kymographs are plotted on a single graph to allow comparison between different populations of tracks

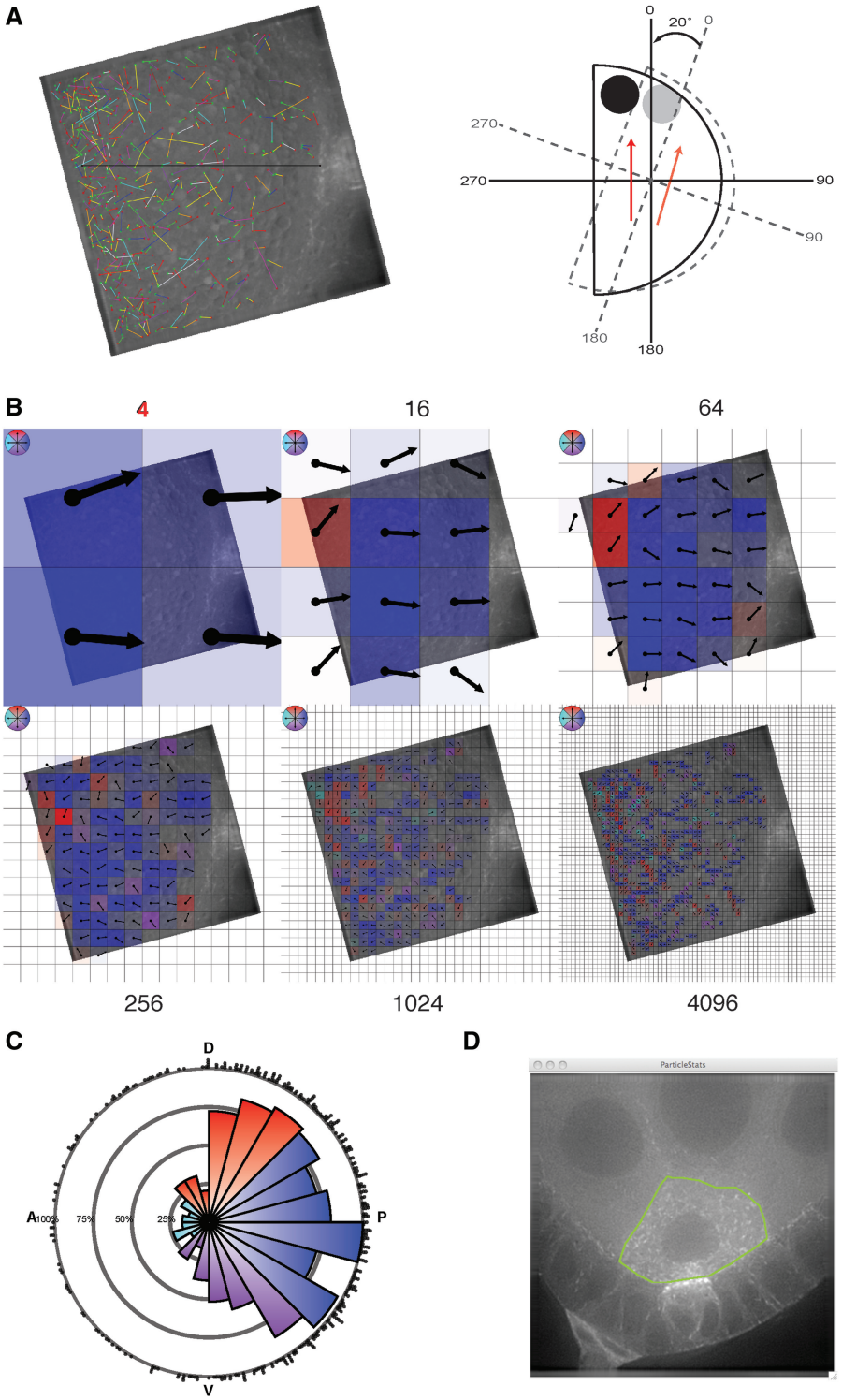

Figure 1. ParticleStats:Directionality. (**A**) The tracked particles are plotted and rotated according to a user defined axis (red arrow). (**B**) Windmaps visually display trends in the directionality of tracked particles. The windmaps are created for a range of square resolutions (4–4096) and are coloured according to the user-defined axis, e.g. dorsal (red), posterior (blue), ventral (purple), anterior (cyan). (**C**) A rose diagram showing the angle of each track around the circumference of the plot. The petals of the rose show angles for tracks in defined angle ranges. (**D**) A screenshot of the simple graphical tool used to generate coordinates for a regions of interest (ROI).

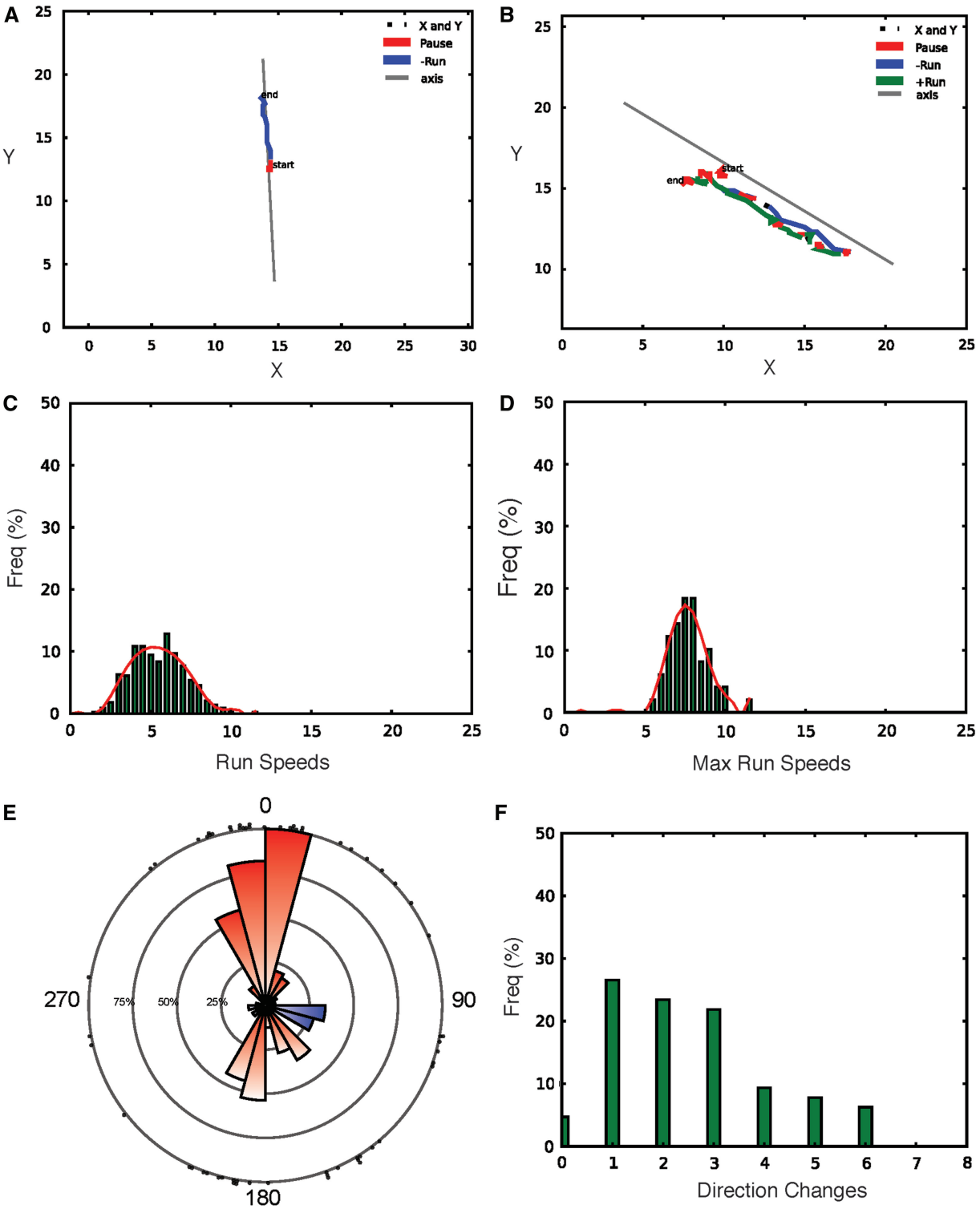

Figure 2. ParticleStats:Compare. (**A** and **B**) Two examples of plots of kinetochore separation. The movements are divided up into runs (+, green; −, blue) and pauses (red) with a user-supplied orientation line (grey). (**C**) A frequency distribution for run speeds, where the runs have been split into overlapping three frame windows. (**D**) The maximum three frame speed is plotted for each run. (**E**) Rose diagram with individual run angles plotted on the circumference, and the petals showing run angle frequencies. (**F**) A frequency distribution of the changes in direction for runs in a set of kinetochore separation examples.

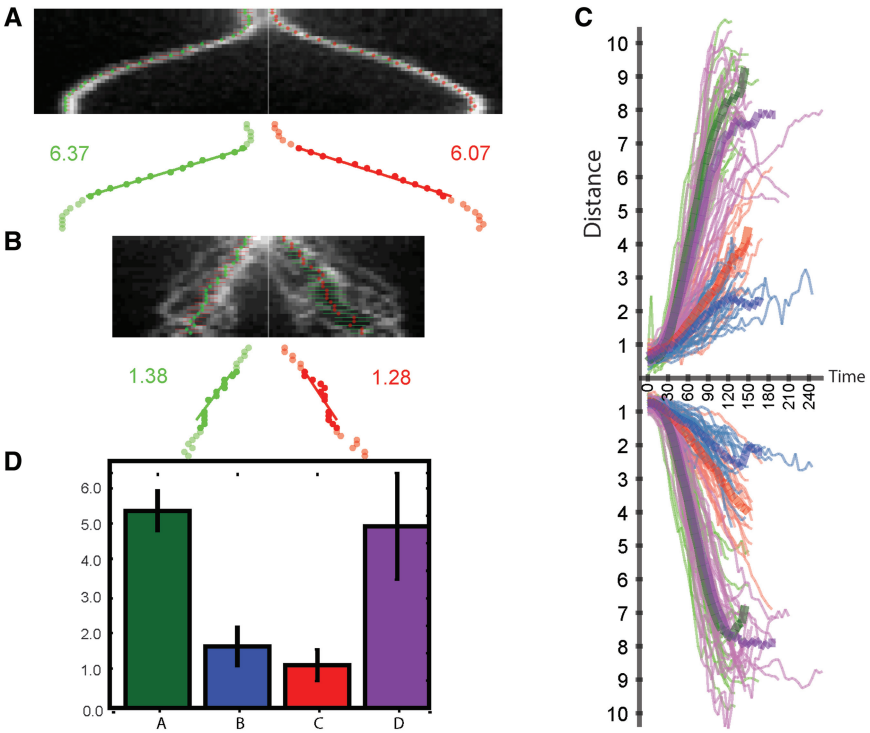

Figure 3. ParticleStats:Kymographs. (**A**) Kymograph of eight aligned kinetochore pairs. Weighted averages of the intensities are used to pick out the kinetochore paths (upper panel) and linear regression is used to determine the speed of the kinetochore separation (lower panel). (**B**) A kymograph showing less synchronous separation of kinetochores. (**C**) A plot of the kinetochore paths for approximately thirty examples of four variants of kinetochore separation experiments. Each of the four variants has an averaged line for the weighted averages. (**D**) A plot of the average speeds for the four variant kinetochore separations with error bars showing weighted standard deviations.

(Figure 3C). The speeds for each of the populations are then plotted along with weighted standard deviation (Figure 3D).

CONCLUSION

A number of open source and commercial particle tracking programmes exist and perform some analysis of the resulting *X*, *Y* coordinates with time. There are also studies performing analyses on tracked data, examples include the use of rose diagrams in a study of myosin motility (16) and kymograph analysis for the microtubule mediated transport of Merlin (17). However, the software for performing these analyses are not made publicly available. Here, we describe ParticleStats, motility analysis tools to tackle the quantitation and statistical analysis of three distinct classes of motility problems in cells, available as a web server and as open source code. ParticleStats is applicable to any study yielding *X* and *Y* coordinates and will have a wide range of possible applications throughout cell biology. First, we have developed ParticleStats:Directionality a new method for the global mapping, display and statistical comparison of fields of orientated fibres or trajectories of moving objects within cells. This has a wide range of applications, ranging from the polarity of MT fibres in any kind of cell as derived from plus end tip growth, to the analysis of cell motility trajectories. Second, ParticleStats:Compare can be applied to many transport phenomena such as motor dependent mRNA particle transport (11). These include, lipid droplet transport (2,18), transport of mitochondria in *Drosophila* motor axons (1,19), neurofilament proteins in squid axoplasm (20), nuclear trafficking of HIV particles (21), influenza viruses (22) and 1D diffusion of proteins along DNA (23) or active transport along axons and dendrites (24,25). Third, ParticleStats:Kymograph was developed to be applicable to a range of applications in addition to the segregation of chromosomes. Such cases include mitochondrial transport (26), protein co-transport (27) and arrangement of actin bundles in *Aplysia* growth cones (28), as well as any kind of one dimensional transport or diffusion phenomena.

FUNDING

Wellcome Trust Senior Research Fellowship (081858 to I.D., R.S.H., R.M.P.); Fundação para Ciência e a Tecnologia of Portugal fellowship (to R.A.O.); Engineering and Physical Sciences Research Council (to G.B.); State Scholarship Foundation of Greece (to G.V.); Medical Research Council and Wellcome Trust (to K.N.). Funding for open access charge: Wellcome Trust Senior Research Fellowship (to I.D.).

Conflict of interest statement. None declared.

REFERENCES

1. Hollenbeck,P.J. and Saxton,W.M. (2005) The axonal transport of mitochondria. *J. Cell Sci.*, **118**, 5411–5419.

2. Gross,S.P., Welte,M.A., Block,S.M. and Wieschaus,E.F. (2000) Dynein-mediated cargo transport in vivo. A switch controls travel distance. *J. Cell Biol.*, **148**, 945–956.
3. Levi,V., Gelfand,V.I., Serpinskaya,A.S. and Gratton,E. (2006) Melanosomes transported by myosin-V in Xenopus melanophores perform slow 35 nm steps. *Biophys. J.*, **90**, L07–L09.
4. Tekotte,H. and Davis,I. (2002) Intracellular mRNA localization: motors move messages. *Trends Genet.*, **18**, 636–642.
5. Jansen,R.P. (2001) mRNA localization: message on the move. *Nat. Rev. Mol. Cell Biol.*, **2**, 247–256.
6. St Johnston,D. (2005) Moving messages: the intracellular localization of mRNAs. *Nat. Rev. Mol. Cell Biol.*, **6**, 363–375.
7. Meignin,C. and Davis,I. (2010) Transmitting the message: intracellular mRNA localization. *Curr. Opin. Cell Biol.*, **22**, 112–119.
8. Jaqaman,K., Loerke,D., Mettlen,M., Kuwata,H., Grinstein,S., Schmid,S.L. and Danuser,G. (2008) Robust single-particle tracking in live-cell time-lapse sequences. *Nat. Methods*, **5**, 695–702.
9. Bullock,S.L., Zicha,D. and Ish-Horowicz,D. (2003) The Drosophila hairy RNA localization signal modulates the kinetics of cytoplasmic mRNA transport. *EMBO J.*, **22**, 2484–2494.
10. Carter,B.C., Shubeita,G.T. and Gross,S.P. (2005) Tracking single particles: a user-friendly quantitative evaluation. *Phys. Biol.*, **2**, 60–72.
11. Vendra,G., Hamilton,R.S. and Davis,I. (2007) Dynactin suppresses the retrograde movement of apically localized mRNA in Drosophila blastoderm embryos. *RNA*, **13**, 1860–1867.
12. Oliveira,R.A., Hamilton,R.S., Pauli,A., Davis,I. and Nasmyth,K. (2010) Cohesin cleavage and Cdk inhibition trigger formation of daughter nuclei. *Nat. Cell Biol.*, **12**, 185–192.
13. Jammalamadaka,S.R. and Sengupta,A. (2001) *Topics in Circular Statistics*. World Scientific, Singapore, London.
14. Wilkie,G.S. and Davis,I. (2001) Drosophila wingless and pair-rule transcripts localize apically by dynein-mediated transport of RNA particles. *Cell*, **105**, 209–219.
15. Bullock,S.L. and Ish-Horowicz,D. (2001) Conserved signals and machinery for RNA transport in Drosophila oogenesis and embryogenesis. *Nature*, **414**, 611–616.
16. Brawley,C.M. and Rock,R.S. (2009) Unconventional myosin traffic in cells reveals a selective actin cytoskeleton. *Proc. Natl Acad. Sci. USA*, **106**, 9685–9690.
17. Bensenor,L.B., Barlan,K., Rice,S.E., Fehon,R.G. and Gelfand,V.I. (2010) Microtubule-mediated transport of the tumor-suppressor protein Merlin and its mutants. *Proc. Natl Acad. Sci. USA*, **107**, 7311–7316.
18. Welte,M.A., Gross,S.P., Postner,M., Block,S.M. and Wieschaus,E.F. (1998) Developmental regulation of vesicle transport in Drosophila embryos: forces and kinetics. *Cell*, **92**, 547–557.
19. Pilling,A.D., Horiuchi,D., Lively,C.M. and Saxton,W.M. (2006) Kinesin-1 and Dynein are the primary motors for fast transport of mitochondria in Drosophila motor axons. *Mol. Biol. Cell*, **17**, 2057–2068.
20. Prahlad,V., Helfand,B.T., Langford,G.M., Vale,R.D. and Goldman,R.D. (2000) Fast transport of neurofilament protein along microtubules in squid axoplasm. *J. Cell Sci.*, **113(Pt 22)**, 3939–3946.
21. McDonald,D., Vodicka,M.A., Lucero,G., Svitkina,T.M., Borisy,G.G., Emerman,M. and Hope,T.J. (2002) Visualization of the intracellular behavior of HIV in living cells. *J. Cell Biol.*, **159**, 441–452.
22. Lakadamyali,M., Rust,M.J., Babcock,H.P. and Zhuang,X. (2003) Visualizing infection of individual influenza viruses. *Proc. Natl Acad. Sci. USA*, **100**, 9280–9285.
23. Gorman,J. and Greene,E.C. (2008) Visualizing one-dimensional diffusion of proteins along DNA. *Nat. Struct. Mol. Biol.*, **15**, 768–774.
24. Bramham,C.R. and Wells,D.G. (2007) Dendritic mRNA: transport, translation and function. *Nat. Rev. Neurosci.*, **8**, 776–789.
25. Thomas,M.G., Martinez Tosar,L.J., Loschi,M., Pasquini,J.M., Correale,J., Kindler,S. and Boccaccio,G.L. (2005) Staufen recruitment into stress granules does not affect early mRNA transport in oligodendrocytes. *Mol. Biol. Cell*, **16**, 405–420.
26. Baloh,R.H., Schmidt,R.E., Pestronk,A. and Milbrandt,J. (2007) Altered axonal mitochondrial transport in the pathogenesis of Charcot-Marie-tooth disease from mitofusin 2 mutations. *J. Neurosci.*, **27**, 422–430.
27. Roy,S., Winton,M.J., Black,M.M., Trojanowski,J.Q. and Lee,V.M.-Y. (2007) Rapid and intermittent cotransport of slow component-b proteins. *J. Neurosci.*, **27**, 3131–3138.
28. Katoh,K., Hammar,K., Smith,P.J.S. and Oldenbourg,R. (1999) Arrangement of radial actin bundles in the growth cone of aplysia bag cell neurons shows the immediate past history of filopodial behavior. *Proc. Natl Acad. Sci. USA*, **96**, 7928–7931.